12WCEE 2000

1934

NONLINEARITY IN OBSERVED AND COMPUTED ACCELEROGRAMS

Ralph J ARCHULETA[1], Luis Fabián BONILLA[2] And Daniel LAVALLÉE[3]

SUMMARY

In this study we present evidence that nonlinearity can be directly observed in acceleration time histories of nonlinear soil response such as Bonds Corner, 1979 Imperial Valley, CA; Wildlife Refuge accelerogram, 1987 Superstition Hills, CA; Kushiro Port station, 1993 Kushiro-Oki, Japan. To understand the causes of these observations we have modeled laboratory tests on sands by applying extended Masing rules for hysteresis that follow general hyperbolic stress-strain relationships. We developed a functional form for the extended Masing rules and incorporated this function into a visco-elastic finite difference code to propagate vertically incident SH-waves in a layered medium. Using a simple pore pressure relationship, we can incorporate the degradation of the shear modulus and the yield stress that result from elevated pore pressure built up during the cyclic response of the material. The simulations show amplitude reduction as well as the shift of the fundamental frequency to lower frequencies as observed on vertical arrays. The synthetic accelerograms show the development of intermittent behavior—high frequency peaks riding on low frequency carrier—as observed in acceleration records. Using the Wildlife Refuge, Kushiro Port, and Port Island borehole arrays, we have modeled the recorded ground motions at the surface and different depths. The synthetic acceleration time histories and response spectra show good agreement with the data. Moreover without liquefaction, nonlinearity produces large strains in the soil with large amplification in the low frequency band of the ground motion.

INTRODUCTION

While nonlinearity in ground motion is often inferred, there are only a few cases where nonlinearity has been directly observed in strong ground motion accelerograms. Moreover quantifying the degree of nonlinearity during strong shaking is difficult because of the many assumptions that are necessary in characterizing the site geology. We will present a new characteristic of accelerograms that we believe is a direct result of nonlinearity in the soil during strong ground shaking. To examine the behavior of the soil during strong shaking we have developed a formulation of nonlinear stress-strain based on the Masing rules. This formulation produces the characteristics associated with nonlinear soil response such as a shift of the fundamental frequency to longer periods, damping, and shear modulus reduction. It also produces the intermittent behavior of the soil in exacerbating the duration, intermittent peaks in acceleration and a shift of low-frequency energy to higher frequency. We will use this formulation to examine case histories of known nonlinear soil response as well as to investigate the role of critical parameters in affecting the soil response.

[1] *Institute for Crustal Studies & Dept. of Geological Sciences, Univ. of California, USA ralph@crustal.ucsb.edu*
[2] *Institute for Crustal Studies & Dept. of Geological Sciences, Univ. of California, USA fabian@crustal.ucsb.edu*
[3] *Institute for Crustal Studies, Univ. of California, Santa Barbara, CA, USA (daniel@crustal.ucsb.edu)*

DATA

Of course one of the clearest examples of nonlinear response are the Port Island borehole records of the 1995 Hyogo-ken Nambu earthquake. While less of a direct observation than borehole recordings, nonlinear response is generally associated with accelerograms that show a pronounced change in frequency content that occurs during or immediately after strong shaking. A classic example of such behavior is the response at Treasure Island (a soft soil site) for the 1989 Loma Prieta earthquake. Fortunately there was an accelerogram recorded on rock about two kilometers away at Yerba Buena Island for comparison (Figure 1). The contrast between the two accelerograms clearly suggests that the Treasure Island site experienced a nonlinear response.

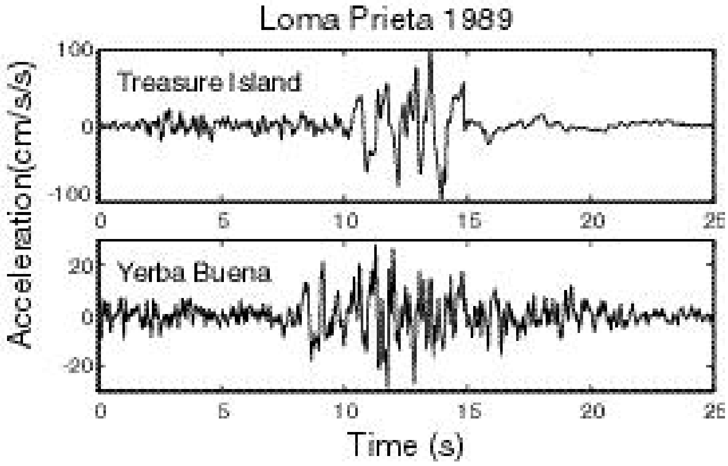

Figure 1. Horizontal accelerograms (north-south) from the 1989 Loma Prieta earthquake recorded at two sites that are within 2.5 kilometers of each other.

Other than borehole observations of strong shaking or in the serendipity situation where accelerograms are recorded at rock and soil sites close to each other, nonlinearity of the soil must be inferred by indirect methods. A basic approach is to compare the transfer function for weak and strong ground motion recorded at the same site. The principal observation one expects for nonlinear response is a shift to longer period of the fundamental frequency of the transfer function. A major difficulty with this approach is finding a reference site. Borehole data provide an excellent baseline for such studies [Satoh *et al*. 1995, 1997]; [Wen *et al*., 1994], but the effect of the downgoing waves must be carefully considered [Steidl *et al*., 1996]. Using data from the 1994 Northridge earthquake Field *et al*. (1996) compared the average amplification of strong and weak shaking for a class of soil sites with that of a few rock sites to infer widespread nonlinear soil response at frequencies between 1.0 and 4.0 Hz. Recently O'Connell (1999) has shown that linear response and scattering of waves in the upper kilometers of the earth's crust can explain much of the same data used by Field and others. Using data from the 1989 Loma Prieta earthquake Idriss, (1990) compared peak accelerations on rock sites compared to soil sites for the same event to infer nonlinear response. Beresnev and Wen (1996) review many of the seismological cases where researchers have inferred nonlinear soil response.

Characteristic Waveform

We have noticed that some strong motion accelerograms have a characteristic waveform that we have associated with nonlinear response [Archuleta, 1998]. One of the most obvious examples of this waveform is clearly observed in the Port Kushiro surface acceleration time history (Figure 2) of the 1993 Kushiro-oki earthquake [Iai *et al*., 1995]. Thorough analysis of this surface record by Iai *et al*. (1995) leaves no doubt that the spiky waveform is the result of nonlinear response of the soil. However, this characteristic waveform was noted much earlier by Porcella, (1980). He pointed out that several USGS accelerograms had this spiky character and "It is hoped that future recordings from these stations will contain some indication of the origin and nature of these high-frequency, large amplitude spikes." He included the Bonds Corner accelerogram for the 15 October 1979 Imperial Valley earthquake (Figure 3), Cerro Prieto accelerogram for the 9 June 1980 northern Mexico earthquake, and four recordings at the left abutment of Long Valley Dam from four M>6 earthquakes in May 1980 near Mammoth Lakes.

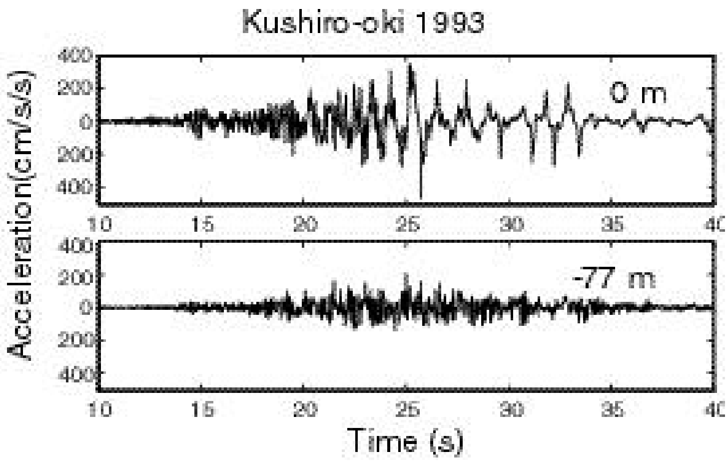

Figure 2. Surface and borehole acceleration time histories for a dense sand deposit during the 1993 Kushiro-oki earthquake. Note the spiky repetitive waveform that dominates the surface recording after 30 seconds.

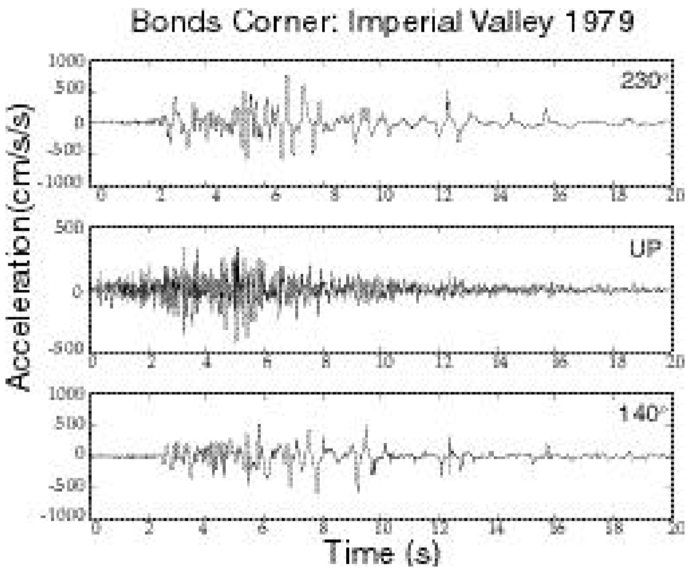

Figure 3. Accelerograms for Bonds Corner recorded during the 1979 Imperial Valley earthquake. Note the spiky acceleration starting around 6 s and coming after the main S waves.

This characteristic waveform is present in the Wildlife Refuge recordings of the 1987 Superstition Hills earthquake [Holzer *et al*., 1989]; [Zeghal and Elgamal, 1994], the fault normal Takatori accelerogram of the 1995 Hyogo-ken Nanbu earthquake [Kamae *et al*., 1998] and the 1994 Northridge accelerogram recorded at Sylmar Converter Station in the Van Norman Dam Complex [Bardet and Davis, 1996]. Certainly this characteristic waveform is a direct consequence of nonlinear soil response at Kushiro Port [Iai *et al*., 1995] and the Wildlife Refuge [Zeghal and Elgamal, 1994]. For the records at the Wildlife Refuge array Zeghal and Elgamal, (1994) were able to associate these spikes in acceleration with episodes of dilatancy in corresponding pore pressure measurements that were simultaneously recorded. In both cases the authors have highlighted the nonlinear dilatant behavior of the soil as the probable cause of the spiky accelerations. The Wildlife Refuge site underwent liquefaction, but the Kushiro Port site did not.

This manifestation of nonlinearity is different from previous observations in that the nonlinearity does not diminish the high frequency nature of the accelerograms or necessarily reduce the peak acceleration. In the case of Bond's Corner the peak acceleration is associated with the peak of one of these characteristic waveforms. The other aspect of the accelerograms is that the nonlinearity extends the duration of strong shaking as opposed to the commonly held view that nonlinearity will reduce the duration, e.g., Treasure Island (Figure 1). This nonlinear effect creates a record that has higher accelerations late in the record that are not related to the source.

Theoretical formulation of the model: Generalized Masing rules

To study and understand the phenomenology of nonlinear soil response to earthquake, we have developed a numerical model that captures the essential physics of nonlinearity in soil. The model formulation includes nonlinear effects such as anelasticity and hysteretic behavior (also known as the memory effect).

The propagation of seismic waves directly depends on the mechanical properties of the material. In a typical geological setting, the shear wave velocity of the sediments increases with depth. Consequently, seismic wave paths are bent toward the earth surface, and hit the surface with almost normal incidence. Empirical results also show that the shear wave dominates the seismic signal. Thus, in a first approximation, the wave propagation can be reduced to a one-dimensional shear wave. The model assumes continuum mechanics and implements a computer-based numerical integration of the one-dimensional shear wave equation of motion with appropriate boundary and initial conditions:

$$\rho \frac{\partial^2 u}{\partial t^2} = \frac{\partial \tau}{\partial z} \tag{1}$$

Here $u(z,t)$ denotes the displacement field perpendicular to the vertical axis at position z and time t, ρ is the unstrained density of the material, and $\tau(z,t)$ is the shear stress. The rheology of the soil describes the stress-strain relationship in terms of the soil properties and parameters. In the hyperbolic model, the nonlinear relation is given by the following equation:

$$\tau = \frac{G_{max}\gamma}{1 + \left| \frac{G_{max}}{\tau_{max}} \gamma \right|^{\alpha}} + \eta \frac{\partial \gamma}{\partial t} \tag{2}$$

where $\gamma(z,t) = \partial u(z,t)/\partial z$ denotes the shear strain, G_{max} is the maximum shear modulus at low strain, τ_{max} is the maximum stress that the material can support in the initial state, and η is the viscosity factor. The parameter α is a constant set to 1.0 in the original hyperbolic model. The first term on the right hand side of Eq. 2 corresponds to the anelastic properties, while the second term corresponds to energy dissipation by viscosity and basically introduces the effect of Q into the computation. Degradation of the soil parameters G_{max} and τ_{max} due to pore pressure is approximated using relationships outlined in Elgamal (1991).

Hysteresis behavior can be implemented with the help of the Masing and extended Masing rules (see Kramer, 1996; for more details and motivation for incorporating the extended Masing rules see Bonilla *et al*., 1998). However, these rules are not enough to constrain the shear stress τ to values not exceeding the parameter τ_{max}. This may happen when the time behavior of the shear strain departs from the simple cyclic behavior. For instance when consecutive extrema of the function $\gamma(t)$ (or turning points) have the same sign, application of the Masing rules lead to an estimated τ corresponding to unphysical situation (that is when the computed stress exceeds the strength of the material). Of course, noncyclic time behavior is common in seismic signals. Inadequacy of the Masing rules to describe the hysteretic behavior of complicated signals has been already pointed out and some remedies have been proposed (e.g., Pyke, 1979 and references therein; Xiaojung, and Zhenpeng, 1993)

The Masing rules consist of a translation and dilatation of the original law governing the strain-stress relationship. While the initial loading of the material is given by the backbone curve $F_{bb}(\gamma)$ (for instance Eq. 2), for the subsequent loadings and unloadings, the strain-stress relationship is given by:

$$\frac{t - t_r}{c_H} = F_{bb}\left(\frac{g - g_r}{c_H}\right) \tag{3}$$

except when the extended Masing rules are applied. The coordinate (g_r, t_r) corresponds to the reversal points in the strain-stress space. In Masing's original formulation, the hysteresis scale factor c_H is equal to 2.0. A first extension to the Masing rules can be obtained by releasing the constrain $c_H = 2$. This parameter controls the shape of the loop in the stress-strain space [Bonilla *et al.*, 1998]. However numerical simulations suggest spurious behavior of t for irregular loading and unloading processes even when extended Masing rules are used. A further generalization of Masing rules is obtained choosing the value of c_H is such way to assure that the path $t(g)$, at a given unloading or reloading, in the strain-stress space will cross the backbone curve. This can be achieved by solving the following relationship:

$$c_H^{(n)} F_{bb}\left(\frac{Sign\left(\frac{dg}{dt}\right)|g_f| - g^{(n)}}{c_H^{(n)}}\right) = F_{bb}\left(Sign\left(\frac{dg}{dt}\right)|g_f|\right) - t^{(n)} \tag{4}$$

$$t^{(n)} = \sum_{i=2}^{n} c_H^{(i-1)} F_{bb}\left(\frac{g^{(i)} - g^{(i-1)}}{c_H^{(i-1)}}\right) + F_{bb}\left(g^{(1)}\right) \tag{5}$$

where $g^{(n)}$ corresponds to the turning point at the n^{th} unloading or reloading (the index n is even at reloading and odd when unloading). The time derivative in Eq. 4 is estimated at time larger –and different- than the time of the last turning point. In this formulation the parameter $c_H^{(n)}$ will have in general different values at different reloadings or unloadings. The value of the hysteresis scale factor is related to the physical properties of the material and one free parameter g_f, the point where the curves intersect in the strain-stress space. The values given to g_f, with $|g^{(1)}| \le |g_f| < \infty$ ($g^{(1)}$ corresponds to the first turning point), controls the amount of energy dissipated through the nonlinear property of the material. More energy is stocked in the material as g_f increases. The limit $g_f \to \infty$ corresponds to the Cundall-Pike hypothesis [Pyke, 1979], while $g_f = g^{(1)}$ is similar to some extent to a method discussed in [Xiaojung, and Zhenpeng, 1993]. A third rule must be supplemented when $|g^{(1)}| < |g_f| < \infty$, which is that the stress-strain relationship is given by the backbone equation each time $|g|$ exceeds $|g_f|$. The Generalized Masing rules can be summarized by the following relation:

$$t(g) = \begin{cases} F_{bb}(g) & g < g^{(1)}, t < t^{(1)} \\ c_H^{(n)} F_{bb}\left(\frac{g - g^{(n)}}{c_H^{(n)}}\right) + t^{(n)} & |g| \le |g_f|, t \ge t^{(1)} \\ F_{bb}(Sign\left(\frac{dg}{dt}\right)g) & |g| \ge |g_f|, t \ge t^{(1)} \end{cases} \tag{6}$$

where $t^{(1)}$ is the time corresponding to the first turning point and $t^{(n)}$ given by Eq. (5) (see Bonilla *et al.*, 1999 for more details and motivation for the Generalized Masing rules).

An illustration of the behavior of the strain-stress curve is shown in Figure 4 for an irregular loading using the Generalized Masing rules and a backbone curve given by Eq. 2. This nonlinear model was used to reproduce the 1987 Superstition Hills M 6.7 earthquake recorded at the Wildlife Refuge. The ground motion was recorded in a borehole sensor located at GL-7.5m and at GL-0m depth. The signals observed at GL-7.5m were propagated to the surface allowing pore pressure build up following a model proposed by Elgamal, (1991). In Figure 5, the computed acceleration at the surface is compared to the observations.

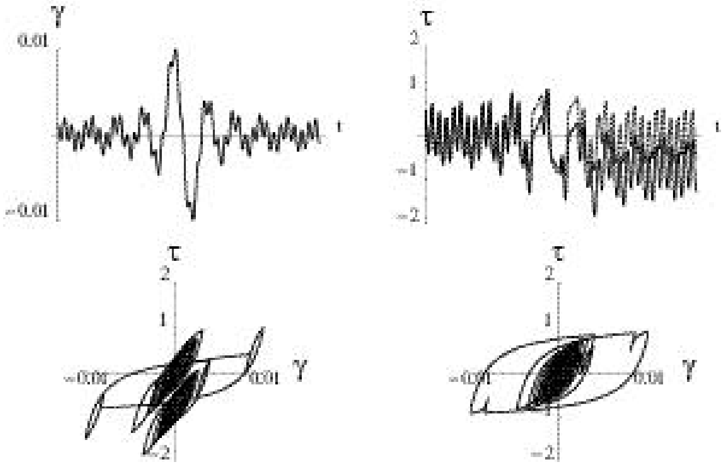

Figure 4. Examples of computed stress time histories following the original Masing rules (solid line), and the model proposed in this study (dashed line). Note how the original Masing rules produce stress that exceeds the maximum strength of the material, in this case 1 kPa.

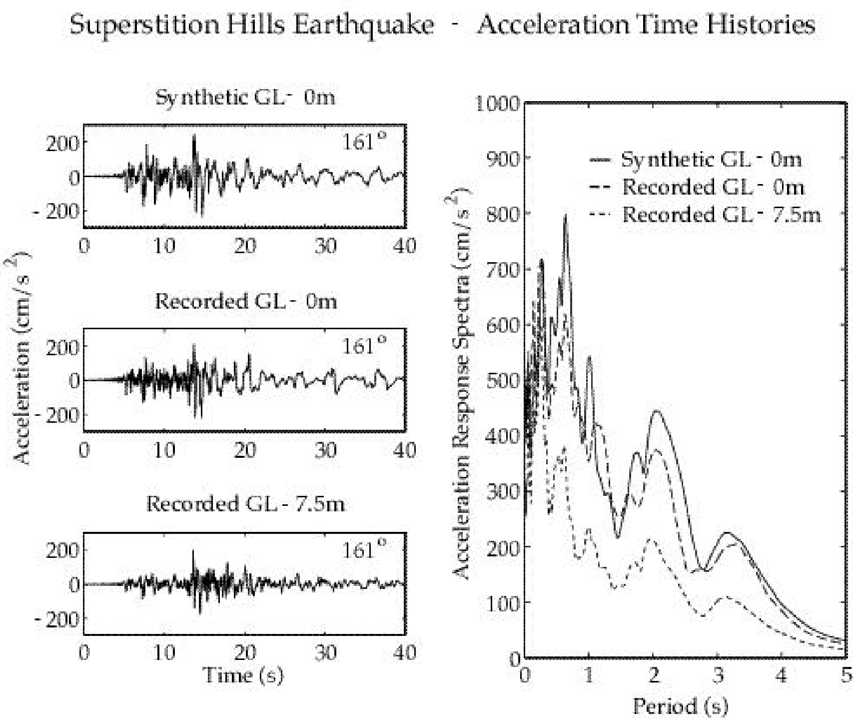

Figure 5. Nonlinear modeling of the 1987 Superstition Hills M 6.7 earthquake recorded at the Wildlife Refuge. On the left side, the observed and synthetic acceleration time histories are plotted for GL-0m depth above the obsereved GL-7.5m recording. On the right side are the corresponding 5% damping response spectra. These curves show a good agreement in both the time domain and for all periods.

CONCLUSIONS

In summary, there is a new direct observation of nonlinearity in soils. This nonlinearity presents itself in the accelerograms as the spiky, nearly repetitive character that is seen in examples such as Bond’s Corner, the Kushiro Port accelerogram, and others named earlier. The numerical solutions demonstrate a shift of the fundamental frequency to a lower frequency as the degree of nonlinearity is increased. There is also an increase in the spectral response for frequencies larger than the fundamental. Nonlinearity produces high frequency, large amplitude acceleration spikes late in the record thereby increasing the duration of the strong shaking. The increase in spectral amplitudes and increased duration of strong shaking are not normally associated with the effects of nonlinearity though different soil models have suggested this effect (e.g., Yu *et al*., 1992). The identification of nearly repetitive, high frequency, large amplitude spikes late in the acceleration time history is another direct indication of nonlinearity in the soil response.

ACKNOWLEDGMENTS

The first author wants to thank S. Iai whose presentation (in January of 1996 at the International Workshop on Site Response) of the Kushiro accelerograms triggered my memory of Porcella's atypical accelerograms. This work was supported by the U. S. Nuclear Regulatory Commission, NRC-04-96-046 and the French Institute de Protection et de Surete Nuclear, #4060-00001217. This paper is ICS contribution No. 0348-96EQ

REFERENCES

Archuleta, R. J. (1998), "Direct observation of nonlinear soil response in acceleration time histories", *Seism. Res. Lett.* 69, pp149.

Bardet, J. P. and Davis, C. (1996), "Engineering observations on ground motion at the Van Norman Complex after the 1994 Northridge earthquake", *Bull. Seism. Soc. Am.* 86 (1B): ppS333-S349.

Beresnev, I. and Wen, K. (1996), "Review: nonlinear soil response--a reality?", *Bull. Seism. Soc. Am.* 86, pp1964-1978.

Bonilla, L. F., Lavallée, D. and Archuleta, R. J. (1998), "Nonlinear Site Response: Laboratory Modeling as a constrain for modeling accelerograms", *Proceeding of the Second International Symposium on the Effects of Surface Geology on Seismic Motion*, Vol. 2, edited by K. Irikura, K. Kudo H. Okada and T. Sasatani, A.A. Balkema: Netherlands, pp793-800.

Bonilla, L. F., Lavallée, D. and Archuleta, R. J. (1999), "A Generalized Hysteresis Model for Masing Rules," in preparation for *Earthquake eng. Struct. Dyn.*

Elgamal, A-W. (1991), "Shear Hysteretic elasto-plastic earthquake response of soil systems," *Earthquake eng. Struct. Dyn.*, 20, pp371-387.

Field, E. H., Johnson, P. A., Beresnev, I. A and Zeng, Y. (1997), "Nonlinear ground-motion amplification by sediments during the 1994 Northridge earthquake", *Nature*. 390, pp599-602.

Holzer, T. L., Youd, T. L. and Hanks, T. C. (1989), "Dynamics of liquefaction during the 1987 Superstition Hills, California, earthquake", *Science* 244, pp56-59.

Iai, S., Morita, T., Kameoka, T., Matsunaga, Y. and Abiko, K. (1995), "Response of a dense sand deposit during 1993 Kushiro-Oki Earthquake", *Soils and Foundations*. 35, pp115-131.

Idriss, I., M. (1990), "Response of soft soil sites during earthquakes," in J. M. Dunca, ed., Proceedings, H. Bolton Seed memorial Symposium, BiTech Publishers, Vancouver, BC, Vol. 2, pp273-289.

Kamae, K., Irikura, K. and Pitarka, A. (1998), "A technique for simulating strong ground motion using hybrid Green's functions", *Bull. Seism. Soc. Am.* 88, pp357-367.

Kramer, S. L. (1996), *Geothechnical Earthquake Engineering*, Prentice Hall, New Jersey.

O'Connell, D. R. H., (1999) "Replication of Apparent Nonlinear Seismic Response with Linear Wave Propagation Models", *Science*, 283, pp2045-2033.

Pyke, R. (1979), "Nonlinear soil model for irregular cyclic loadings", *J. of the Geotech. Engrg. Div.*, 105 (6), pp715-726.

Porcella, R. L. (1980), "Atypical accelerograms recorded during recent earthquakes", *Seismic Engineering Program Report. May-August: 1980, Geological Survey Circular 854-B*, pp1-7.

Satoh, T., Horike, M., Takeuchi, Y., Uetake, T. and Suzuki, H. (1997), "Nonlinear behavior of scoria soil sediments evaluated from borehole records in Eastern Shizuoka Prefecture, Japan", *Earthquake Eng. Struct. Dyn.* 26, pp781-795.

Satoh, T., Sato, T. and Kawase, H. (1995), "Nonlinear behavior of soil sediments identified by using borehole records observed at the Ashigara Valley, Japan", *Bull. Seism. Soc. Am.* 85, pp1821-1834.

Steidl, J. H., Tumarkin, A. G. and Archuleta, R. J. (1996), "What is a reference site?", *Bull. Seism. Soc. Am.*. 86, pp1733-1748.

Wen, K., Beresnev, I. and Yeh, Y. T. (1994), "Nonlinear soil amplification inferred from downhole strong seismic motion data", *Geophys. Res. Lettrs.* 21, pp2625-2628.

Xiaojung, L. and Zhenpeng, L. (1993), "Dynamic skeleton corve of soil stress-strain relation under irregular cyclic loading", *Earthquake research in China*, 7, pp469-477.

Yu, G., Anderson, J. G. and Siddharthan, R. (1992), "On the characteristics of nonlinear soil response", *Bull. Seism. Soc. Am.*. 83, pp218-244.

Zeghal, M. and Elgamal, A-W. (1994), "Analysis of site liquefaction using earthquake records", *J. Geotech. Eng.* 120, pp996-1017.